Acoustic streaming-based calibration of ultrasound transducers

dos Santos, Djalma Simões; Baldini, Leonardo; Vos, Hendrik J.; Verweij, Martin D.; de Jong, Nico; van Neer, Paul L.M.J.

DOI
10.1016/j.apacoust.2024.109863

Publication date
2024

Document Version
Final published version

Published in
Applied Acoustics

Citation (APA)
dos Santos, D. S., Baldini, L., Vos, H. J., Verweij, M. D., de Jong, N., & van Neer, P. L. M. J. (2024). Acoustic streaming-based calibration of ultrasound transducers. *Applied Acoustics*, *217*, Article 109863. https://doi.org/10.1016/j.apacoust.2024.109863

Applied Acoustics 217 (2024) 109863

Contents lists available at ScienceDirect

Applied Acoustics

journal homepage: www.elsevier.com/locate/apacoust

Acoustic streaming-based calibration of ultrasound transducers

Djalma Simões dos Santos [a,*], Leonardo Baldini [a], Hendrik J. Vos [a,b], Martin D. Verweij [a,b], Nico de Jong [a,b], Paul L.M.J. van Neer [a,c]

[a] Laboratory of Medical Imaging, Department of Imaging Physics, Delft University of Technology, Delft, The Netherlands
[b] Department of Biomedical Engineering, Thoraxcenter, Erasmus Medical Center, Rotterdam, The Netherlands
[c] Netherlands Organisation for Applied Scientific Research (TNO), The Hague, The Netherlands

ARTICLE INFO

Keywords:
Ultrasound transducer
Transfer function
Safety
Sensitivity
Acoustic streaming
Reciprocity

ABSTRACT

The accurate determination of the transfer function of ultrasound transducers is important for their design and operational performance. However, conventional methods for quantifying the transfer function, such as hydrophone measurements, radiation force balance, and pulse-echo measurements, are costly and complex due to specialized equipment required. In this study, we introduce a novel approach to estimate the transfer function of ultrasound transducers by measuring the acoustic streaming velocity generated by the transducer. We utilize an experimental setup consisting of a water tank with a millimeter scale, an ink-filled syringe, and a camera for recording the streaming phenomenon. Through streaming velocity measurements in the frequency range from 2 to 8 MHz, we determined the transfer function of an unfocused circular transducer with a center frequency of 5 MHz and a radius of 5.6 mm. We compared the performance of our method with hydrophone and pulse-echo measurements. At the center frequency, we measured a transmit efficiency of 1.9 kPa/V using the streaming approach, while hydrophone and pulse-echo measurements yielded transmit efficiencies of 2.1 kPa/V and 1.8 kPa/V, respectively. These findings demonstrate that the proposed method for estimating the transfer function of ultrasound transducers achieves a sufficient level of accuracy comparable to pulse-echo and hydrophone measurements.

1. Introduction

The characterization of the pressure field transmitted by ultrasound transducers is a critical aspect of their design process. This process is crucial for validating models, optimizing design parameters, evaluating the manufacturing process, and investigating acoustic phenomena that may affect the transducer's behavior in practice [1]. Furthermore, pressure field characterization is essential to facilitate the maintenance of transducers used in various applications, particularly in the medical field. As the operating characteristics of ultrasound transducers tend to change over time and usage with an average lifespan [2], concerns may arise regarding the effectiveness and safety of these transducers [3]. Therefore, it is imperative to establish test routines to periodically evaluate the performance of ultrasound transducers and ensure their compliance with national and international standards [4].

An important aspect in assessing the performance of an ultrasound transducer is determining its transmit transfer function, also known as transmit efficiency, which is a frequency-dependent quantity defined as the ratio of the output acoustic pressure at the transducer's surface to the input voltage on its electrodes [5]. Various methods have been proposed to estimate the transmit efficiency of the transducer, with the standard approach involving the use of a calibrated hydrophone to record the time-varying acoustic pressure generated by the transducer at specified locations using an *xyz*-positioning stage. Although this method is convenient, it can be costly as hydrophone calibration needs to be performed annually at an accredited laboratory [6–8]. Another common technique for measuring the acoustic output of ultrasound transducers is the use of radiation force balances. This method measures the acoustic radiation force produced when ultrasound is incident upon an absorbing target [9]. However, this technique has its drawbacks, as it is expensive, challenging to operate, and highly sensitive to noise and vibrations [10].

Alternative methods for estimating the transducer transfer function are based on the reciprocity technique [11]. Dang et al. [12] introduced a model-based approach that employs three transducers in a pitch-catch configuration and only requires electrical measurements such as voltage and current. This method enables the determination of both the

* Corresponding author.
E-mail address: D.SimoesdosSantos@tudelft.nl (D.S. dos Santos).

https://doi.org/10.1016/j.apacoust.2024.109863
Received 4 September 2023; Received in revised form 27 November 2023; Accepted 5 January 2024
Available online 13 January 2024

magnitude and phase of the transfer function. However, this is a relatively complex and time-consuming process that involves the use of three distinct setups, requiring careful realignments between changes in setup. Lopez-Sanchez et al. [13] proposed a simplified version of the aforementioned method, which uses a single pulse-echo setup and relies solely on electrical measurements to determine the magnitude and phase of the transfer function. However, this method has a drawback as the magnitude of the transfer function is somewhat affected by the settings of the driving source at lower frequencies. Van Neer et al. [5] proposed a method that employs a pulse-echo setup along with complex electrical impedance measurements. This method can determine the absolute transfer function with a high degree of accuracy and is relatively straightforward. However, it requires the use of an impedance analyzer, which is an expensive device that may not always be accessible. Matte et al. [7] proposed an alternative method for estimating the absolute transfer function by using an uncalibrated hydrophone together with pressure field simulations. This method requires an iterative algorithm to match the measured levels of harmonics with the simulated harmonic distortion coefficient. A limitation of this approach is that it considers only the second harmonic in the calculations, which results in a sharp increase in estimation error at high-pressure levels.

Recently, a few studies have investigated the transmit characterization of transducers through a phenomenon called acoustic streaming. Acoustic streaming refers to the steady flow induced by the ultrasound transducer in the propagating medium [14]. By measuring the streaming velocity, which is directly related to the acoustic power emitted by the transducer, it becomes possible to estimate the acoustic pressure generated by the transducer. Hariharan et al. [15] and Slama et al. [16] utilized acoustic streaming to characterize high-intensity focused ultrasound (HIFU) transducers, while Tan et al. [17] applied it to characterize an ultrasonic thruster. To track the acoustic streaming motion and predict the intensity field of the transducer, these studies utilized particle image velocimetry (PIV). Although this approach successfully characterized the acoustic output of the transducers, it's important to note that it involves complex experimental setups and requires sophisticated algorithms to solve the seeding particle velocity.

In this paper, we introduce a streaming-based method for determining the transmit transfer function of ultrasound transducers. The key advantage of our approach is that it offers a simpler setup compared to the previous studies that utilize PIV to track streaming motion. Instead, we employ ink as a tracer and use a digital camera to measure the induced streaming velocity in water. To validate the effectiveness of the proposed method, we compared its performance with two other well-established methods: hydrophone and pulse-echo measurements [5,18].

2. Theory

Acoustic streaming refers to the consistent movement or steady flow of a fluid induced by the propagation of acoustic waves. This is a nonlinear effect that can be described using the general equations of hydrodynamics, namely the continuity Eq. (1) and the Navier-Stokes Eq. (2).

$$\frac{\partial \rho}{\partial t} + \nabla \cdot \rho \nu = 0 \quad (1)$$

$$\rho\left(\frac{\partial \nu}{\partial t} + \nu \cdot \nabla \nu\right) = -\nabla p + \left(\zeta + \frac{4}{3}\eta\right)\nabla\nabla\cdot\nu - \eta\nabla\times\nabla\times\nu \quad (2)$$

where p is the pressure, ρ the density, ν the velocity, and ζ and η are, respectively, the bulk and the shear viscosity coefficients of the fluid [14,19]. By combining Eq. (1) and (2), we obtain:

$$\frac{\partial(\rho\nu)}{\partial t} + \rho(\nu\cdot\nabla)\nu + \nu\nabla\cdot\rho\nu = -\nabla p + \left(\zeta + \frac{4}{3}\eta\right)\nabla\nabla\cdot\nu - \eta\nabla\times\nabla\times\nu \quad (3)$$

The phenomenon of acoustic streaming can be divided into two components: a linear oscillation component, which is dominated by the fluid's compressibility, and a steady flow component, which is governed by the fluid's viscosity. In this context, it is assumed that the time scales of the harmonic oscillations and the steady flow differ significantly from each other [20]. To implement this idea, Nyborg [21,22] introduced expansions of the pressure, density, and velocity in terms of successively higher-order approximations:

$$\begin{aligned} p &= p_0 + p_1 + p_2 \\ \rho &= \rho_0 + \rho_1 + \rho_2 \\ \nu &= 0 + \nu_1 + \nu_2 \end{aligned} \quad (4)$$

where the subscript 0 denotes the state of the undisturbed fluid, 1 represents the first-order approximations that oscillate in time with frequency ω, and 2 indicates the second-order approximations that are time-independent [20,23]. The term ν_2 is the streaming velocity that we seek. Using the higher-order approximations and taking the time average of Eq. (3), Nyborg obtained a governing equation for the acoustic streaming, which may be written as:

$$F = -\nabla p_2 + \left(\zeta + \frac{4}{3}\eta\right)\nabla\nabla\nu_2 - \eta\nabla\times\nabla\times\nu_2 \quad (5)$$

with

$$\mathrm{F} = \rho_0\langle(\nu_1\cdot\nabla)\nu_1 + \nu_1(\nabla\cdot\nu_1)\rangle \quad (6)$$

and the symbol $\langle X\rangle$ denotes the time average of X at a fixed point in space [19,22]. Note that F depends only on first-order quantities and is a known function, while the right-hand side of Eq. (5) contains unknown second-order terms. This means that the force F is equivalent to an external force driving the second-order system.

For an exponentially attenuating plane wave, this force is called the acoustic radiation force F_{rad} and can be expressed as:

$$\mathrm{F_{rad}} = \frac{2\alpha \mathrm{I_{TA}}}{\mathrm{c}} \quad (7)$$

where α is the absorption coefficient, I_{TA} is the local time-average acoustic intensity, and c is the longitudinal sound speed in the medium [24–27].

Nowicki et al. [28,29] obtained the solution for the axial component of the streaming velocity for the case of a plane acoustic wave generated by an unfocused circular transducer, which is given by:

$$\nu_{2z}(0,0,z) = \frac{\alpha I_{TA} r^2}{\eta c}\int_0^\infty e^{-2\alpha r s}\left[\sqrt{1+\left(\frac{z}{r}-s\right)^2} - \sqrt{1+\left(\frac{z}{r}+s\right)^2} + \left(\frac{z}{r}+s\right) - \left|\frac{z}{r}-s\right|\right]ds \quad (8)$$

where r is the radius of the transducer, I_{TA} is the time-averaged intensity at the surface of the transducer, and s is the integration variable on the propagation axis z.

Eq. (8) establishes a relationship between the streaming velocity and the acoustic intensity at the transducer surface. Therefore, by measuring the velocity of the streaming flow along the axial axis, one can calculate the acoustic pressure generated at the surface of the transducer, provided the medium properties and the transducer effective radius are known. It is important to note that this analysis is based on the assumption that the streaming jet maintains a steady, laminar flow within an infinite medium. This implies that there is no interaction between the acoustic beam and the surrounding walls, thereby eliminating the presence of an acoustic boundary layer in the problem. Under these conditions, the flow dynamics are primarily governed by a balance between the effects of viscosity, inertia, and the acoustic radiation force [30].

3. Materials and methods

3.1. Acoustic streaming measurements

Fig. 1(a) depicts the experimental setup used for generating acoustic streaming, comprising a circular transducer (V309, Olympus NDT, Waltham, MA, USA), placed in a water tank labeled with a millimeter grid to enable distance measurement. The transducer used in the experiment had a center frequency of 5 MHz and an effective radius of 5.6 mm, which was determined by comparing the simulated radiation pattern of a piston model with experiments [31]. To drive the transducer, we employed an arbitrary function generator (AWG; 33521A, Agilent Technologies, Inc., Santa Clara, CA, USA), which was configured to generate a sine wave burst with a peak amplitude of 0.2 V into a 50 Ω load. This burst had a duty factor τ of 0.7 and operated at a pulse repetition frequency PRF of 100 Hz. The excitation frequency f ranged from 2 to 8 MHz, incrementing in steps of 1 MHz. The number of cycles n applied for each excitation frequency was determined by:

$$n = \tau \cdot \frac{f}{PRF} \tag{9}$$

The AWG output was then amplified by a 50 dB power amplifier (2100L, ENI, Inc., Rochester, NY, USA) and connected to the transducer. To measure the voltage at the transmitting transducer at various frequencies, a digital oscilloscope (DSO-X 2022A, Agilent Technologies, Inc., Santa Clara, CA, USA) was utilized.

To track the axial streaming velocity, we injected 10 ml of ink (Quink, Parker Pen Company, Boulogne-Billancourt, France) into the water using a syringe and recorded the resulting flow using a digital camera (PowerShot SX620 HS, Canon, Inc., Ota, Japan) at a rate of 30 frames per second. Special care was taken to avoid external vibrations and to ensure that the ink jet flowed undisturbed along the axial axis of the transducer. Multiple videos were recorded at each excitation frequency to minimize variability and random errors. The recorded videos were transferred to a computer for processing, and the streaming velocity was measured by analyzing sequential frames from the videos. To account for optical refraction effects in the readout of the millimeter scale, a comparison was made between the size of the millimeter scale immersed in water and behind the water tank wall. We observed a factor of 0.56 difference between the two cases, which was then utilized to correct for refraction in the streaming velocity measurements. To prevent acoustic reflections, we placed an ultrasound absorber at the wall of the water tank, directly in front of the transducer.

The time-averaged intensity I_{TA} at the transducer surface was then calculated using Eq. (8) with $\alpha = 2.5 \times 10^{-4}$ Np/cm/MHz^2, $\eta = 1$ mPa·s, and $c = 1470$ m/s for water at 20 °C.

Next, the peak pressure p_0 at the surface of the transducer was calculated by:

$$p_0 = \left(\sqrt{\frac{2\rho c I_{TA}}{\tau}} \right) \tag{10}$$

where ρ is 997 kg/m^3.

Once the peak pressure was obtained for each excitation frequency, we calculated the transmit transfer function T_t of the transducer by:

$$T_t(\omega) = \frac{p_0(\omega)}{V(\omega)} \tag{11}$$

where V is the peak voltage measured over the transducer.

For reciprocal transducers, the transmit and receive transfer functions are related by the complex spherical wave reciprocity [11]. Using the expression derived by van Neer et al [5,18], the receive transfer function T_r of a circular transducer can be expressed as:

$$\frac{T_r(\omega)}{T_t(\omega)} = \frac{2 \cdot Z(\omega) \cdot A}{\rho \cdot c} \tag{12}$$

where Z is the electrical impedance of the transducer and $A = \pi r^2$ is its surface area.

3.2. Hydrophone measurements

Fig. 1(b) depicts the experimental setup utilized for obtaining the transmit transfer function via hydrophone measurements, which is described by van Neer et al [5]. A calibrated hydrophone (SN3800, Precision Acoustics Ltd., Dorchester, UK) with a diameter of 0.2 mm was positioned 160 mm away from the transducer surface. An xyz-stage was used to ensure proper alignment. The transducer was excited with a 1-cycle sine wave with a peak amplitude of 5 V generated by an AWG (33250A, Agilent Technologies, Inc., Santa Clara, CA, USA) with the

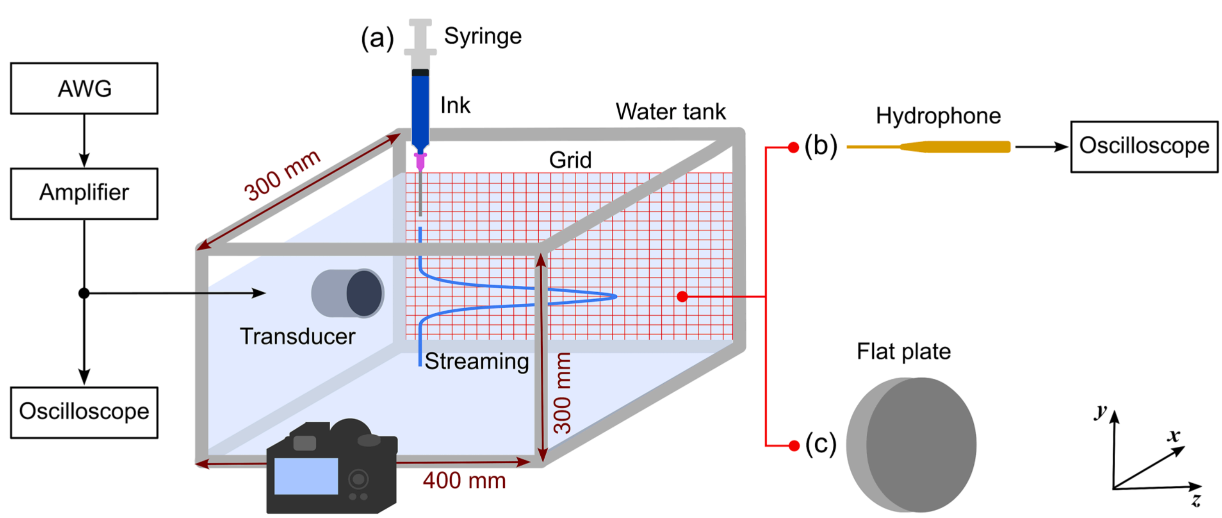

Fig. 1. Experimental setup for transmit transfer function estimation with different methods (not drawn to scale). (a) Acoustic streaming. (b) Hydrophone measurements. (c) Pulse-echo measurements.

output impedance set to 50 Ω. Both the voltage at the transmitting transducer and the output voltage of the hydrophone were digitized by an oscilloscope (DSO-X 4054A, Agilent Technologies, Inc., Santa Clara, CA, USA) and transferred to a computer for processing. The transmit transfer function of the transducer derived from hydrophone measurements was calculated by:

$$T_t(\omega) = \frac{V_{hydr}(\omega)}{V(\omega)\cdot T_{hydr}(\omega)\cdot D(\omega)\cdot \alpha(\omega)} \tag{13}$$

where V_{hydr} is the Fourier transform of the voltage produced by the hydrophone, V is the Fourier transform of the voltage measured over the transducer, T_{hydr} is the transfer function of the hydrophone, D is the diffraction correction function for the transducer [32], and α is the attenuation.

3.3. Pulse-echo measurements

Fig. 1(c) shows the experimental setup for deriving the transmit transfer function from pulse-echo measurements according to the method introduced by van Neer et al [18,33]. Prior to conducting the pulse-echo measurements, the complex electrical impedance of the transducer submerged in water was recorded using an impedance analyzer (4294A, Agilent Technologies, Inc., Santa Clara, CA, USA). As a reflector, we used a cylindrical steel plate with a diameter of 200 mm and a thickness of 80 mm placed at a distance of 160 mm from the transducer. The transducer was driven using a 1-cycle sine wave with a peak amplitude of 5 V generated by an AWG (33250A, Agilent Technologies, Inc., Santa Clara, CA, USA) with the output impedance set to 50 Ω. Both the transmitting voltage measured over the transducer and the received echo signal were digitized by an oscilloscope (DSO-X 4054A, Agilent Technologies, Inc., Santa Clara, CA, USA) with its input impedance set to 1 MΩ. The transmit transfer function derived from pulse-echo measurements was calculated by:

$$T_t(\omega) = \sqrt{\frac{V_{open}(\omega)\cdot\rho\cdot c}{2\cdot Z(\omega)\cdot A\cdot V(\omega)\cdot D(\omega)\cdot\alpha(\omega)\cdot R}} \tag{14}$$

where V_{open} is the Fourier transformed open circuit voltage over the transducer (in reception), ρ is the density of the medium, c is the sound speed in the medium, Z is the electrical impedance of the transducer, A is the area of the transducer, V is the Fourier transform of the voltage over the transducer (in transmission), D the diffraction correction function for the transmitting transducer to the flat plate and back [32], α is the attenuation, and R is the reflection coefficient of the reflector (0.94 for steel).

4. Results

Fig. 2(a) shows the graph just after the ink is injected into the water but before the ultrasound transducer is turned on. The ink jet is situated at an axial of 55 mm from the transducer. Since no streaming is generated, the ink jet sinks to the bottom of the tank in a straight line. In Fig. 2 (b – d) the transducer is activated, and the acoustic streaming generated is clearly visible in the tracer. As time goes by, the wavefront of the streaming moves away from the transducer and its displacement can be easily tracked with the scale behind it. By analyzing the ink displacement at multiple frames, the instantaneous streaming velocity can be measured.

Fig. 3 shows the comparison between the streaming velocities obtained from simulations and measurements along the axial line, utilizing a 5 MHz excitation. Based on the measured streaming velocities, we estimate a source peak pressure of about 30 kPa at the transducer surface, which was subsequently used in the simulations. Notably, the measured and simulated velocities demonstrate a good agreement within the range of 100 to 200 mm, where the velocity stabilizes. The slightly lower values measured at 40 and 80 mm are likely due to both inertia [30] and suboptimal alignment between the camera and the direction of the ink jet.

In Fig. 4, the measured electrical impedance of the transducer when

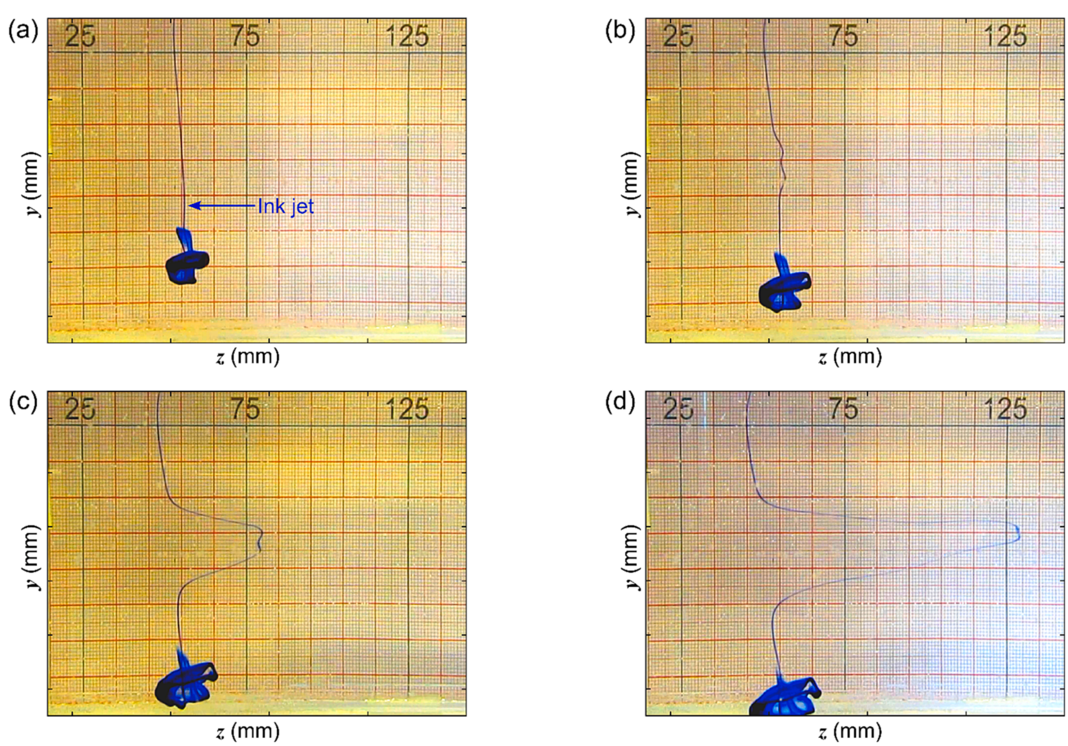

Fig. 2. Streaming flow moving the ink jet at different instants in time with a 5 MHz excitation. (a) Time = 11.67 s. (b) Time = 13.33 s. (c) Time = 15.00 s. (d) Time = 16.67. The scale on the back indicates the axial distance from the transducer surface.

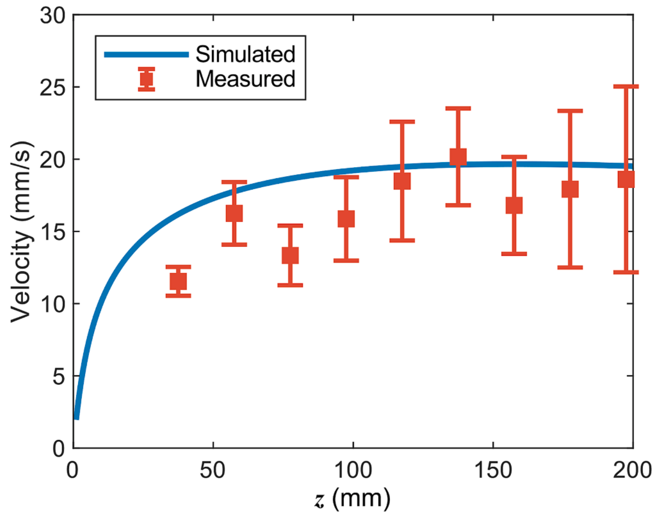

Fig. 3. Simulated and measured streaming velocity along the axial axis with a 5 MHz excitation and a source peak pressure of 30 kPa. The error bars represent the mean values ± one standard deviation of the measured values.

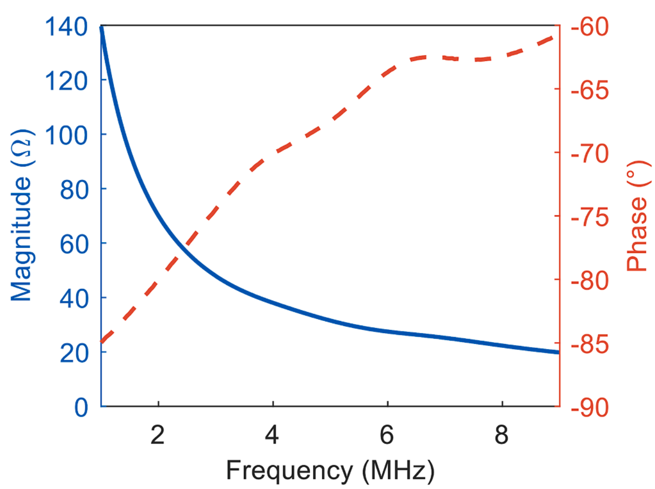

Fig. 4. Measured electrical impedance magnitude (solid line) and phase (dashed line) of the transducer.

submerged in water is shown. As observed, the impedance magnitude demonstrates a gradual decrease across frequencies. A magnitude of approximately 40 Ω is measured near the center frequency of the transducer.

The transmit and the receive transfer functions of the transducer derived using the various methods are shown in Fig. 5(a and b), respectively. At the central frequency of 5 MHz, the transmit efficiency estimated from streaming measurements is 1.9 kPa/V. Comparatively, via hydrophone and pulse-echo measurements, we obtained transmit efficiencies of 2.1 kPa/V and 1.8 kPa/V respectively. Regarding the receive transfer function, we measured a sensitivity of 8.0 μV/Pa through streaming measurements, 9.0 μV/Pa through hydrophone measurements, and 7.7 μV/Pa through pulse-echo measurements at 5 MHz. Overall, the transfer functions obtained from acoustic streaming are in agreement with pulse-echo measurements. At lower frequencies, however, they tend to have lower values compared to hydrophone measurements.

5. Discussion

Hydrophone, pulse-echo measurements, and radiation force balances are standard methods for quantifying the acoustic output of ultrasound transducers. However, these approaches often come with drawbacks such as high costs, complexity, and the requirement for frequent calibration or specialized equipment. In this paper, we introduce an alternative method for evaluating the transfer function of ultrasound transducers utilizing acoustic streaming. By measuring the axial streaming velocity generated by the transducer, we can estimate its acoustic power (similar to the approach of a radiation force balance), and further provide a means to calculate its absolute transmit efficiency. By incorporating impedance measurements, we can determine the receive sensitivity of the transducer, assuming the reciprocity principle. In addition to its inherent simplicity and cost-effectiveness, the proposed method offers the potential to characterize transducers in various environments without requiring extensive modifications to the measurement setup, as long as the medium properties and the effective radius of the transducer are known.

In this study, all water parameters were based on values reported in the literature on ultrasonic waves in water [34,35], except for the speed of sound, which was directly measured. Similar values for water properties have been used in previous studies involving acoustic streaming in water [29,36–38]. Note that, it is assumed in this context that the addition of ink did not alter the inherent properties of the water. Should the experiment be conducted in a different medium, the work of Moudjed et al. may offer valuable insights into establishing a relationship between the streaming velocity in various liquids and the velocity obtained in water [30].

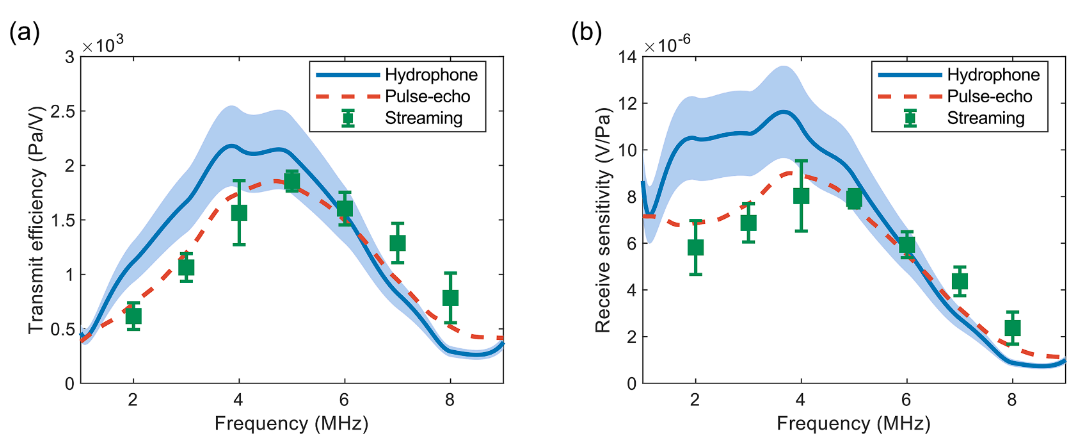

Fig. 5. Transducer transfer function derived from different methods. (a) Transmit efficiency. (b) Receive sensitivity. The error bars represent the mean values ± one standard deviation of the streaming measurements. The shaded areas represent the uncertainty of the hydrophone calibration.

To obtain reliable measurements, it is important to address key aspects of the setup and minimize potential sources of error. First and foremost, external vibrations must be prevented to avoid disturbances in the water and the resulting streaming flow. Within our setup, we observed that certain devices, such as the amplifier, the AWG, and the computer, generated significant vibrations. To minimize their impact, we isolated the water tank on a separate bench, effectively reducing the influence of these vibrations. Additionally, it is crucial to acknowledge that the pumping action of the syringe inherently creates vibrations that can disrupt the streaming flow. To mitigate any unwanted displacement caused by the pumping, we secured the syringe in a holder and ensured that only the needle was submerged in the water, minimizing disturbances to the system. Another potential source of vibration is the push-button of the camera used for recording the streaming. To eliminate manual disturbances, we opted for remote triggering of the camera.

The estimation of the streaming velocity is susceptible to various types of errors. Firstly, it is essential to ensure precise alignment and propagation of the tracer along the axial axis during measurements, as the streaming velocity equation is applicable solely to the axial line. This is particularly important because the side view photos shown in Fig. 2 do not provide information about the lateral position (along the x-direction) of the streaming flow. To address this, incorporating a camera with a top view can be highly beneficial. Secondly, it is worth noting that the approach used for velocity estimation, which involved a scale affixed to the wall of the water tank, is prone to refraction effects and parallax error. Parallax arises when there is a misalignment between the camera, the tracer, and the scale, resulting in inaccuracies. We estimated the refraction correction by measuring a ruler placed on the axial axis. To minimize parallax error, we ensured that the camera was positioned perpendicular to the grid and directly in front of the location where velocity was being estimated. If the streaming velocity is estimated at various positions along the axial line, as in Fig. 3(a), it is advisable to adjust the camera position accordingly to avoid any angled perspectives. Lastly, it is important to measure the streaming velocity a few seconds after activating the ultrasound transducer. This is done to ensure that the flow reaches a steady state and to minimize the influence of inertia on the measurements [15,16]. Note that we conducted velocity measurements at longer intervals after activating the transducer (30 and 45 s) and observed no changes in streaming velocities. This suggests that the flow reached a steady state. Alternatively, the steady-state time could be predicted through numerical calculations, as presented by Hariharan et al [15].

The performance of the proposed method was evaluated by comparing it with hydrophone and pulse-echo measurements. Overall, all three methods provide satisfactory accuracy for absolute transfer function measurements. The transfer functions shown in Fig. 5 demonstrate a similar trend for all three methods, both in transmit and receive modes. Particularly at 5 MHz, they exhibit a relatively good level of agreement, indicating that they are interchangeable and that the selection of the method should be based on specific requirements and practical considerations. When comparing the transmit efficiency derived from streaming measurements with pulse-echo measurements at 5 MHz, an error of 5.5 % is observed, while an error of 9.5 % is obtained when comparing streaming with hydrophone measurements (the uncertainty of the hydrophone calibration is $\pm$17 %). At lower frequencies, the streaming and pulse-echo methods diverge slightly from the hydrophone measurements. Lower frequencies pose challenges as the streaming velocities become low and the ink dissolves in water over a long period of time, making accurate measurements difficult. At higher frequencies, the slight differences between the curves are probably caused by the inaccuracy of estimation of the attenuation coefficient.

6. Conclusion

This paper demonstrates a novel approach for estimating the absolute transfer function of an ultrasound transducer by measuring the velocity of the acoustic streaming it generates. The method was evaluated and compared with hydrophone and pulse-echo measurements. The results showed that our method yields similar outcomes, with an error of 9.5 % compared to hydrophone measurements and an error of 5.5 % compared to pulse-echo measurements at the center frequency. The proposed approach offers an alternative solution for characterizing ultrasound transducers and opens up possibilities for characterization in a wider range of scenarios, particularly in situations where traditional equipment is not accessible due to cost or complexity constraints. In a clinical or industrial environment, the pressure field produced by an ultrasound transducer can be estimated with nothing more than a small water tank, a ruler, and a stopwatch.

CRediT authorship contribution statement

Djalma Simões dos Santos: Conceptualization, Data curation, Formal analysis, Investigation, Methodology, Validation, Visualization, Writing – original draft, Writing – review & editing. **Leonardo Baldini:** Formal analysis, Investigation, Methodology, Writing – review & editing. **Hendrik J. Vos:** Formal analysis, Funding acquisition, Investigation, Project administration, Supervision, Validation, Writing – review & editing. **Martin D. Verweij:** Formal analysis, Investigation, Project administration, Supervision, Validation, Writing – review & editing. **Nico de Jong:** Conceptualization, Formal analysis, Funding acquisition, Project administration, Supervision, Validation, Writing – original draft, Writing – review & editing. **Paul L.M.J. van Neer:** Conceptualization, Data curation, Formal analysis, Funding acquisition, Investigation, Methodology, Project administration, Supervision, Writing – original draft, Writing – review & editing.

Declaration of competing interest

The authors declare that they have no known competing financial interests or personal relationships that could have appeared to influence the work reported in this paper.

Data availability

Data will be made available on request.

Funding

This research is part of the UltraXtreme project (project number P17-32), which is financed by the Netherlands Organization for Scientific Research (NWO).

References

[1] D. S. Dos Santos et al., "Automated Characterization of Matrix Transducer Arrays using the Verasonics Imaging System," in 2022 IEEE International Ultrasonics Symposium (IUS). IEEE. Oct. 2022. 1–4. doi: 10.1109/IUS54386.2022.9957544.

[2] C. Papageorgiou and T. Laopoulos, "Self-calibration of ultrasonic transducers in an intelligent data acquisition system," in *Proceedings of the 2nd IEEE International Workshop on Intelligent Data Acquisition and Advanced Computing Systems: Technology and Applications, IDAACS 2003*, IEEE, 2003, pp. 2–6. doi: 10.1109/IDAACS.2003.1249504.

[3] FDA, "Marketing Clearance of Diagnostic Ultrasound Systems and Transducers," Rockville, MD, USA. 2019.

[4] Roy C. Preston, *Output Measurements for Medical Ultrasound*. London: Springer London, 1991. doi: 10.1007/978-1-4471-1883-1.

[5] van Neer PLMJ, Matte G, Sijl J, Borsboom JMG, de Jong N. Transfer functions of US transducers for harmonic imaging and bubble responses. Ultrasonics 2007;46(4): 336–40. https://doi.org/10.1016/j.ultras.2007.05.002.

[6] IEC 62127-1:2013., "Ultrasonics – Hydrophones – Part 1: Measurement and characterization of medical ultrasonic fields up to 40 MHz," Geneva, Switzerland. 2013.

[7] Matte GM, Borsboom JMG, van Neer P, de Jong N. Estimating Acoustic Peak Pressure Generated by Ultrasound Transducers from Harmonic Distortion Level Measurement. Ultrasound Med Biol 2008;34(9):1528–32. https://doi.org/10.1016/j.ultrasmedbio.2008.03.003.

[8] "OndaSonics. Frequently Asked Questions." Accessed: Jun. 20, 2023. [Online]. Available: https://www.ondasonics.com/applications/faqs/.

[9] Swamy KM, Keil FJ. Ultrasonic power measurements in the milliwatt region by the radiation force float method. Ultrason Sonochem 2002;9(6):305–10. https://doi.org/10.1016/S1350-4177(02)00087-1.

[10] Xing J, Chen J. Design of a Thermoacoustic Sensor for Low Intensity Ultrasound Measurements Based on an Artificial Neural Network. Sensors 2015;15(6): 14788–808. https://doi.org/10.3390/s150614788.

[11] Bobber RJ. General Reciprocity Parameter. J Acoust Soc Am 1966;39(4):680–7. https://doi.org/10.1121/1.1909941.

[12] Dang C, Schmerr Jr LW, Sedov A. Ultrasonic Transducer Sensitivity and Model-Based Transducer Characterization. Res Nondestr Eval 2003;14(4):203–28. https://doi.org/10.1007/s00164-002-0006-5.

[13] Lopez-sanchez A, Schmerr L. Determination of an ultrasonic transducer's sensitivity and impedance in a pulse-echo setup. IEEE Trans Ultrason Ferroelectr Freq Control 2006;53(11):2101–12. https://doi.org/10.1109/TUFFC.2006.150.

[14] Eckart C. Vortices and streams caused by sound waves. Phys Rev 1948;73(1): 68–76. https://doi.org/10.1103/PhysRev.73.68.

[15] Hariharan P, Myers MR, Robinson RA, Maruvada SH, Sliwa J, Banerjee RK. Characterization of high intensity focused ultrasound transducers using acoustic streaming. J Acoust Soc Am 2008;123(3):1706–19. https://doi.org/10.1121/1.2835662.

[16] R. B. H. Slama, B. Gilles, M. Ben Chiekh, and J. C. Bera, "Characterization of focused-ultrasound-induced acoustic streaming," *Exp Therm Fluid Sci*, vol. 101, no. March 2018, pp. 37–47, Jan. 2019, doi: 10.1016/j.expthermflusci.2018.10.001.

[17] A. C. H. Tan and F. S. Hover, "Correlating the Ultrasonic Thrust force with acoustic streaming Velocity," in *2009 IEEE International Ultrasonics Symposium*, IEEE, Sep. 2009, pp. 2627–2630. doi: 10.1109/ULTSYM.2009.5442075.

[18] van Neer PLMJ, Vos HJ, de Jong N. Reflector-based phase calibration of ultrasound transducers. Ultrasonics 2011;51(1):1–6. https://doi.org/10.1016/j.ultras.2010.05.001.

[19] Robert T. Beyer, *Nonlinear Acoustics*. United States. Naval Ship Systems Command. 1974.

[20] Möller D, Hilsdorf T, Wang J, Dual J. Acoustic streaming used to move particles in a circular flow in a plastic chamber. AIP Conf Proc 2012:775–8. https://doi.org/10.1063/1.3703295.

[21] Nyborg WLM. "Acoustic Streaming" 1965:265–331. https://doi.org/10.1016/B978-0-12-395662-0.50015-1.

[22] Nyborg WL. Acoustic Streaming due to Attenuated Plane Waves. J Acoust Soc Am 1953;25(1):68–75. https://doi.org/10.1121/1.1907010.

[23] Wu J, Du G. Acoustic streaming generated by a focused Gaussian beam and finite amplitude tonebursts. Ultrasound Med Biol 1993;19(2):167–76. https://doi.org/10.1016/0301-5629(93)90008-C.

[24] Doherty J, Trahey G, Nightingale K, Palmeri M. Acoustic Radiation Force Elasticity Imaging in Diagnostic Ultrasound. IEEE Trans Ultrason Ferroelectr Freq Control 2013;60(4):685–701. https://doi.org/10.1109/TUFFC.2013.2617.

[25] Palmeri M, Sharma A, Bouchard R, Nightingale R, Nightingale K. A Finite-Element Method Model of Soft Tissue Response to Impulsive Acoustic Radiation Force. IEEE Trans Ultrason Ferroelectr Freq Control 2005;13(14–15):1133–45. https://doi.org/10.1016/j.micinf.2011.07.011.

[26] Bercoff J, Tanter M, Fink M. Supersonic shear imaging: a new technique for soft tissue elasticity mapping. IEEE Trans Ultrason Ferroelectr Freq Control 2004;51(4): 396–409. https://doi.org/10.1109/TUFFC.2004.1295425.

[27] dos Santos DS, Cardoso FM, Furuie SS. Two-dimensional ultrasonic transducer array for shear wave elastography in deep tissues: a preliminary study. Research on Biomedical Engineering 2020;36(3):277–89. https://doi.org/10.1007/s42600-020-00068-6.

[28] Nowicki A, Kowalewski T, Secomski W, Wójcik J. Estimation of acoustical streaming: theoretical model, Doppler measurements and optical visualisation. Eur J Ultrasound 1998;7(1):73–81. https://doi.org/10.1016/S0929-8266(98)00020-2.

[29] Nowicki A, Secomski W, Wójcik J. Acoustic streaming: Comparison of low-amplitude linear model with streaming velocities measured by 32-MHz Doppler. Ultrasound Med Biol 1997;23(5):783–91. https://doi.org/10.1016/S0301-5629(97)00005-7.

[30] Moudjed B, Botton V, Henry D, Ben Hadid H, Garandet J-P. Scaling and dimensional analysis of acoustic streaming jets. Phys Fluids 2014;26(9):Sep. https://doi.org/10.1063/1.4895518.

[31] Schmerr LW. "FUNDAMENTAL MODELS AND MEASUREMENTS FOR ULTRASONIC NONDESTRUCTIVE EVALUATION SYSTEMS", in Ultrasonic and Advanced Methods for Nondestructive Testing and Material Characterization. WORLD SCIENTIFIC 2007:3–31. https://doi.org/10.1142/9789812770943_0001.

[32] Goldstein A, Gandhi DR, O'Brien WD. Diffraction effects in hydrophone measurements. IEEE Trans Ultrason Ferroelectr Freq Control 1998;45(4):972–9. https://doi.org/10.1109/58.710571.

[33] P. L. M. J. van Neer, H. J. Vos, M. G. Danilouchkine, and N. de Jong, "Simple method for measuring phase transfer functions of transducers," in *2010 IEEE International Ultrasonics Symposium*, IEEE, Oct. 2010, pp. 1454–1457. doi: 10.1109/ULTSYM.2010.5935890.

[34] J. M. M. Pinkerton, "The Absorption of Ultrasonic Waves in Liquids and its Relation to Molecular Constitution," *Proceedings of the Physical Society. Section B*, vol. 62, no. 2, pp. 129–141, Feb. 1949, doi: 10.1088/0370-1301/62/2/307.

[35] Liebermann LN. The Second Viscosity of Liquids. Phys Rev 1949;75(9):1415–22. https://doi.org/10.1103/PhysRev.75.1415.

[36] Kamakura T, Sudo T, Matsuda K, Kumamoto Y. Time evolution of acoustic streaming from a planar ultrasound source. J Acoust Soc Am 1996;100(1):132–8. https://doi.org/10.1121/1.415948.

[37] H. Mitome, "The mechanism of generation of acoustic streaming," *Electronics and Communications in Japan (Part III: Fundamental Electronic Science)*, vol. 81, no. 10, pp. 1–8, Oct. 1998, doi: 10.1002/(SICI)1520-6440(199810)81:10<1::AID-ECJC1>3.0.CO;2-9.

[38] Frenkel V, Gurka R, Liberzon A, Shavit U, Kimmel E. Preliminary investigations of ultrasound induced acoustic streaming using particle image velocimetry. Ultrasonics 2001;39(3):153–6. https://doi.org/10.1016/S0041-624X(00)00064-0.